

7-2018

Recognition of Regional Water Table Patterns for Estimating Recharge Rates in Shallow Aquifers

Troy E. Gilmore

University of Nebraska - Lincoln, gilmore@unl.edu


Vitaly A. Zlotnik

University of Nebraska-Lincoln, vzlotnik1@unl.edu

Mason Johnson

University of Nebraska - Lincoln, johnson121@unl.edu

Follow this and additional works at: <http://digitalcommons.unl.edu/natrespapers>

 Part of the [Natural Resources and Conservation Commons](#), [Natural Resources Management and Policy Commons](#), and the [Other Environmental Sciences Commons](#)

Gilmore, Troy E.; Zlotnik, Vitaly A.; and Johnson, Mason, "Recognition of Regional Water Table Patterns for Estimating Recharge Rates in Shallow Aquifers" (2018). *Papers in Natural Resources*. 747.
<http://digitalcommons.unl.edu/natrespapers/747>

This Article is brought to you for free and open access by the Natural Resources, School of at DigitalCommons@University of Nebraska - Lincoln. It has been accepted for inclusion in Papers in Natural Resources by an authorized administrator of DigitalCommons@University of Nebraska - Lincoln.

Published in *Groundwater*, 2018

doi: 10.1111/gwat.12808

Copyright © 2018 National Groundwater Association; published by John Wiley & Sons.

Used by permission.

Submitted November 2017; accepted June 2018; published July 2018.

Recognition of Regional Water Table Patterns for Estimating Recharge Rates in Shallow Aquifers

Troy E. Gilmore,¹ Vitaly Zlotnik,² and Mason Johnson³

1 Conservation and Survey Division, School of Natural Resources, University of Nebraska–Lincoln, 3310 Holdrege Street, Lincoln NE 68583-0996.

Corresponding author: gilmore@unl.edu

2 Department of Earth and Atmospheric Sciences, University of Nebraska–Lincoln, Lincoln, NE 68588-0340

3 Conservation and Survey Division – School of Natural Resources, University of Nebraska–Lincoln, 3310 Holdrege Street, Lincoln, NE 68583-0996

A new, simple approach for estimating groundwater recharge from groundwater table contours by recognizing and quantifying their patterns.

Abstract

We propose a new method for groundwater recharge rate estimation in regions with stream-aquifer interactions, at a linear scale on the order of 10 km and more. The method is based on visual identification and quantification of classically recognized water table contour patterns. Simple quantitative analysis of these patterns can be done manually from measurements on a map, or from more complex GIS data extraction and curve fitting. Recharge rate is then estimated from the groundwater table contour parameters, streambed gradients, and aquifer transmissivity using an analytical model for groundwater flow between parallel perennial streams. Recharge estimates were obtained in three regions (areas of 1500, 2200, and 3300 km²) using available water table maps produced by different methods at different times in the area of High Plains Aquifer in Nebraska. One region is located in the largely undeveloped Nebraska Sand Hills area, while the other two regions are located at a transition

zone from Sand Hills to loess-covered area and include areas where groundwater is used for irrigation. Obtained recharge rates are consistent with other independent estimates. The approach is useful and robust diagnostic tool for preliminary estimates of recharge rates, evaluation of the quality of groundwater table maps, identification of priority areas for further aquifer characterization and expansion of groundwater monitoring networks prior to using more detailed methods.

Introduction

Groundwater recharge rate is a critical control on water resources because it influences groundwater quantity and quality (Böhlke 2002; Healy and Cook 2002; Scanlon et al. 2002; Healy and Scanlon 2010). Estimates of groundwater recharge rates are difficult to make, have high uncertainty and exhibit significant spatial variability (Healy and Scanlon 2010). Use of multiple methods with different spatial resolution (e.g., Healy and Scanlon 2010; Hornero et al. 2016) is not always possible due to complexity of various techniques.

In this study we develop and apply a new simple method for estimating groundwater recharge directly from recognition of regional groundwater table patterns. The pattern recognition aspect of the approach allows for quick, preliminary visual assessment, and the complexity of application can range from measurement of pattern dimensions on a map, to GIS-based extraction of elevation data and numerical analysis of patterns. The model is based on an idealized aquifer-stream system with several limiting assumptions and provides a diagnostic tool for recharge assessment prior to developing more complex models (e.g., Haitjema 2006). Examples of water table contour patterns that may be analyzed include water table contours near gaining or losing streams (Winter et al. 1998), which are well recognized in modeling literature (Anderson and Woessner 1992; Haitjema 1995).

Among the many methods to determine groundwater recharge rates (Scanlon et al. 2002; Huet et al. 2016), relatively few use water table elevation data (Healy and Cook 2002), and none directly quantify rates from pattern recognition as described above. The most common approach that uses water table elevation data is the water table fluctuation method, which requires high temporal resolution groundwater

level data (e.g., 1 h intervals), estimates of specific yield, and is applicable at a spatial scale on the order of meters (Scanlon et al. 2002). Crosbie et al. (2005) used a time series approach and precipitation records to extend the temporal scale of the water table fluctuation method to multiple events, while hybrid approaches (Sophocleous 1991; Park 2012) have combined the water table fluctuation approach with other methods to reduce uncertainty. Vijay et al. (2007) used a GIS-based approach for analyzing relationships between groundwater mounding and recharge. Other methods that directly rely on water table elevations include analytical models (e.g., Su 1994) and transfer-function models (e.g., Wu et al. 1997).

In Nebraska, USA, groundwater-level change maps are published annually (e.g., Young et al. 2016) and used to evaluate the sustainability of groundwater use by observing short- and long-term increases or declines in water table elevation at watershed-to regional scales. The two most recent statewide water table maps (Flowerday et al. 1998; Korus et al. 2013) exhibit salient groundwater flow patterns near streams that have been observed previously (e.g., Stoertz and Bradbury 1989; Lin and Anderson 2003; Lin et al. 2008; Rossman 2015), but such patterns have not been used explicitly to specifically quantify groundwater recharge. One benefit of this study is to increase the quantitative value of these mapping efforts (and those undertaken in other areas).

The objective of this study is to present new methodology that utilizes water table patterns for estimation of groundwater recharge rates (including, e.g., recharge from natural precipitation, enhanced recharge under irrigated lands [from applied water and precipitation], and leakage from irrigation canals or intermittent stream channels). The new approach requires water table map contours, the slope of two streams, and aquifer transmissivity. With contour analyses by GIS, these results can be applied for diagnostic regional-scale (e.g., 10^3 km^2) recharge estimation, assessment of the quality of water table mapping, identification of priority areas for further aquifer characterization, and expansion of groundwater monitoring networks.

Theory

Problem: Groundwater Flow Between Two Streams

We considered groundwater flow between two roughly parallel, perennial (gaining) headwater streams, such as the streams that cut through vegetated dunes in the Nebraska Sand Hills (Figure 1).

Multiple configurations for the two streams were evaluated. In the simplest case, the geometry of two headwater streams was represented by a model where both streams start at the same elevation, parallel in a plane view, and have the same stream slope (Figure 2a). Other configurations are possible, where each stream has its specific slope I_L or I_R (Figure 2b), or additional slant upstream is characterized by a slope I_U (Figure 3c).

Water table contours between the two streams can be qualitatively and quantitatively explained by groundwater recharge between two streams that act as drains (Winter et al. 1998, p. 9, figures 8 and 9); they are well recognized in modeling literature (Stoertz and Bradbury 1989; Anderson and Woessner 1992, p. 155, figure 5.4; Haitjema 1995, p. 346-347, figure 6.32 and 6.33). Their shape is controlled by the balance between groundwater recharge and the ambient groundwater flow associated with stream morphology (stream slope).

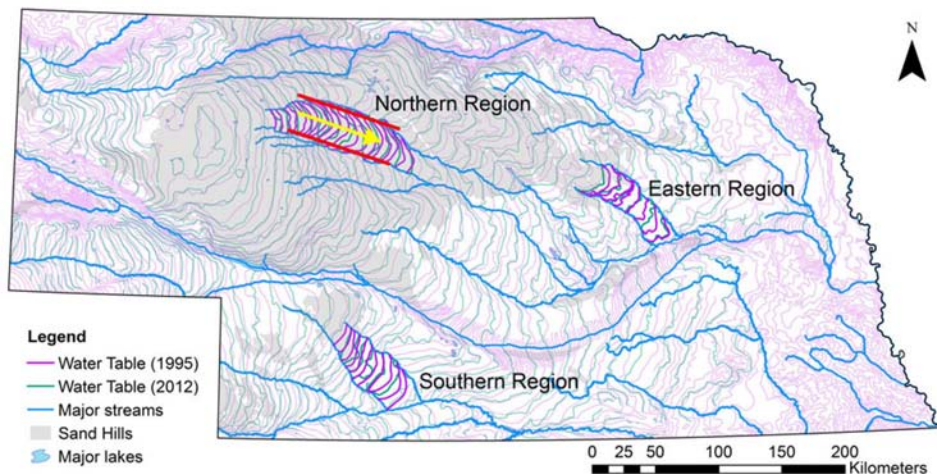


Figure 1. Example of two streams (two red segments), and general direction of groundwater flow (yellow arrow) shown on superimposed water table maps for Nebraska. Note that contour lines (equipotentials) evolve from nearly straight lines at the western edge of the highlighted region to a consistent parabolic shape toward the eastern portion of the region.

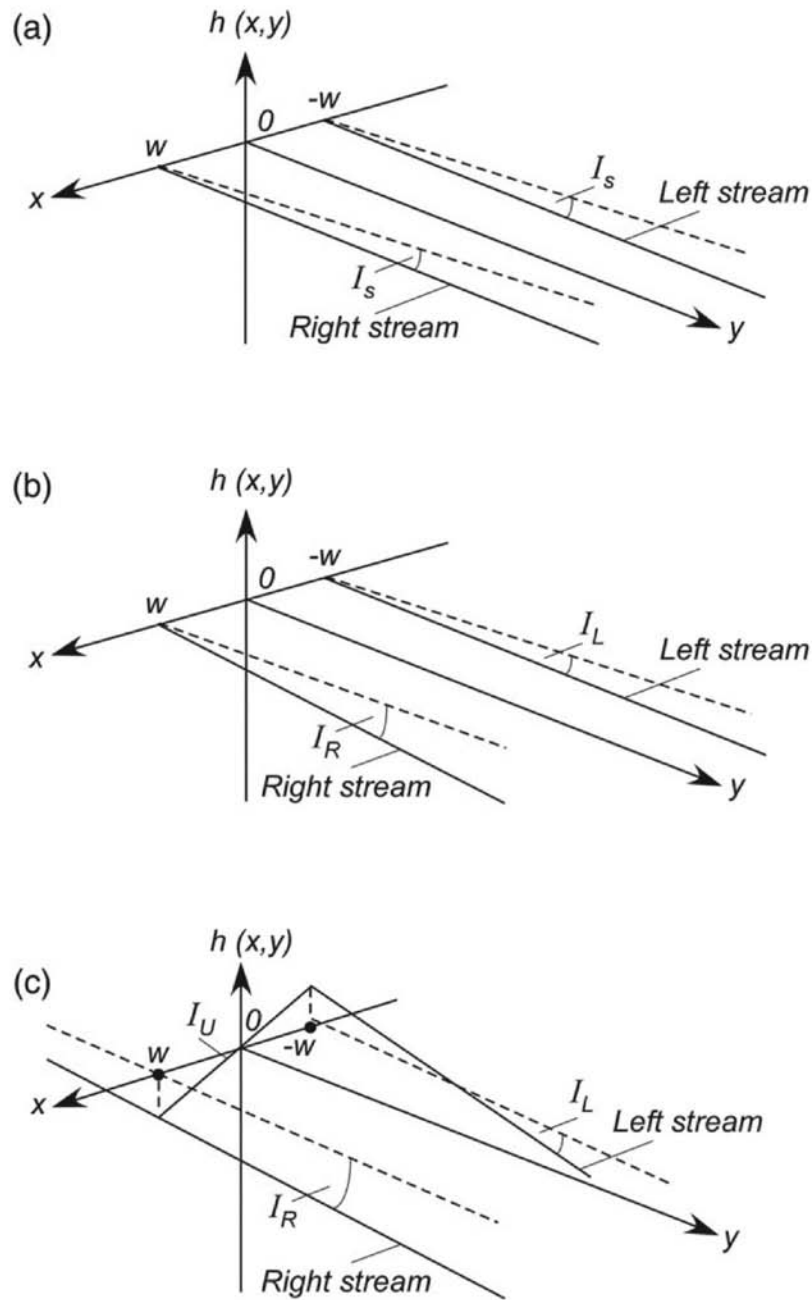


Figure 2. Spatial arrangement of streams in three dimensional: (a) two parallel streams that start at the same elevation; (b) two non-parallel streams that start at the same elevation; (c) two non-parallel streams that start at different elevations. Stream positions and slopes are shown relative to horizontal dashed lines projected on the $h(x,y)$ - x plane and/or x - y plane.

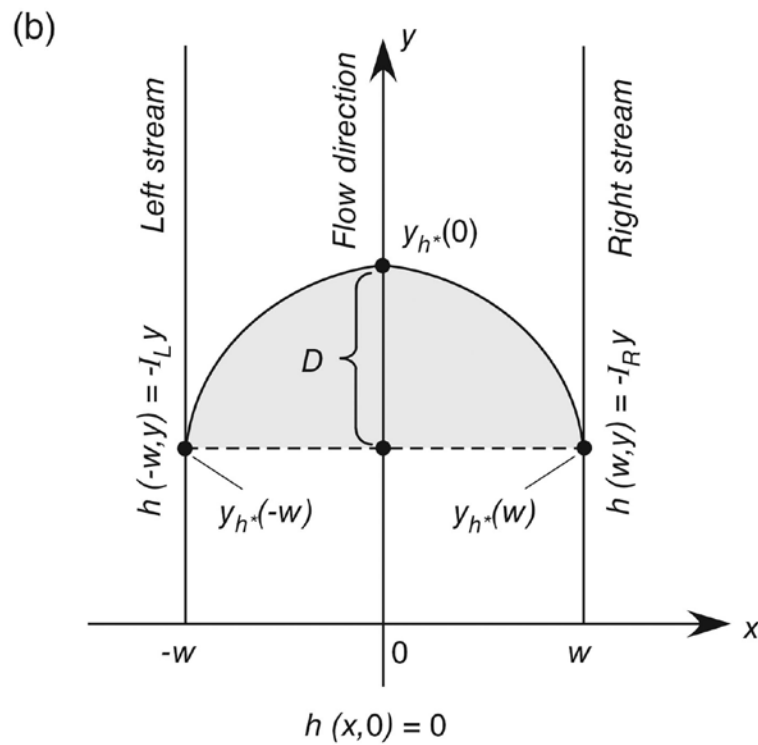
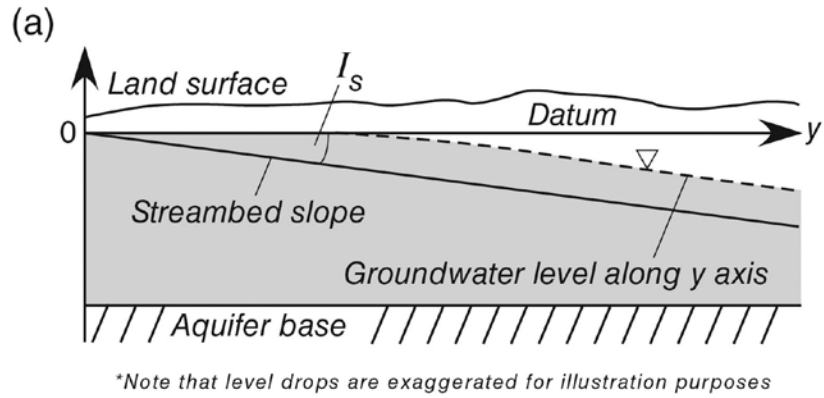


Figure 3. Groundwater flow domain in the unconfined aquifer (a) cross section along the y -axis, and (b) plane view. Stream slopes for left and right streams are labeled differently for generality and consistency with Figure 2. Area under the parabola A is shown in gray.

Base Case Solution: Flow Between Two Parallel Streams

Most commonly, slopes of both streams are identical, and $I_L = I_R = I_S$, and they start at the same elevation $I_U = 0$, which is the base case (Figure 2a). Therefore, we consider head distribution between two parallel streams with the following assumptions:

- The aquifer is unconfined (Figure 3a), homogeneous, isotropic, and the linearized Boussinesq equation for 2-D steady-state groundwater flow (Bear 1972) is applicable. The bottom of the aquifer is assumed to be horizontal (Figure 3).
- Axis y is located at even distances w between streams (Figure 3b).
- Groundwater flow in a domain $-w < x < w$; $0 < y < \infty$ in longitudinal direction y occurs between left and right streams that are separated by a distance $2w$ (Figure 3).
- Transmissivity T and recharge R are uniform in the domain.
- Water table contours (equipotentials) are straight lines at $y = 0$. They acquire identical curvilinear shape downstream at distances $y \gg 2w$.

Of course, the detailed assumptions limit the applicability of the model to hydrogeological settings that reasonably approximate the idealized aquifer-stream system.

The following boundary value problem for the head $h(x, y)$ with datum at the stream upstream level (Figure 2a) is as follows:

$$T \left(\frac{\partial^2 h}{\partial x^2} + \frac{\partial^2 h}{\partial y^2} \right) = -R, \quad -w < x < w; \quad 0 < y < \infty \quad (1)$$

$$h(x, 0) = 0, \quad -w < x < w \quad (2)$$

$$h(\pm w, y) = -I_S \cdot y, \quad 0 < y < \infty \quad (3)$$

In general, local water table slopes will follow the slope of streams along the centerline and in areas further away from the headwaters:

$$\lim_{y \rightarrow \infty} \frac{\partial h(x, y)}{\partial y} = -I_S, \quad -w < x < w \quad (4)$$

The solution can be presented as a sum of two components (e.g., Bruggeman 1999, p. 294, Equation 354.06).

$$h(x, y) = H(x, y) + s(x, y) \quad (5)$$

where term $H(x, y)$ is linear function of y and quadratic function of x ,

$$H(x, y) = \frac{R}{2T}(w^2 - x^2) - I_s y \quad (6)$$

and $s(x, y)$ is a correction

$$s(x, y) = -\frac{16Rw^2}{\pi^3 T} \sum_{n=0}^{\infty} \frac{(-1)^n \cos(\gamma_n x)}{(2n+1)^3} e^{-\gamma_n y}$$

$$\gamma_n = \frac{\pi(2n+1)}{2w} \quad (7)$$

The function $s(x, y)$ in a domain ($-w < x < w$; $0 < y < \infty$) decays rapidly along the y -axis due the presence of exponential terms. The largest deviation of $h(x, y)$ from $H(x, y)$ occurs on the y -axis at $x = 0$, $y = 0$. Analyses in Appendix A show that the correction $s(x, y)$ can be neglected at distances $y > 0.5w$, where $s(x, y)/s(0, 0) < 0.01$ (i.e., the error is on the order of 1% or less). It is also important to note that water levels are changing linearly with increasing distance y downstream according to Equation 6, or along lines parallel to the y -axis ($x = 0$).

Therefore, the function $H(x, y)$ represents the water table configuration away from the upstream boundary:

$$h(x, y) \approx H(x, y), \quad y \gg w \quad (8)$$

Explicit Equation for Contour Patterns

A water table contour (or equipotential) with head h_* can be defined as follows:

$$h(x, y) = h_* \quad (9)$$

and according to Equation 8, the implicit equation for equipotentials away from the upstream boundary is as follows:

$$h(x, y) \approx H(x, y) = h_* = \frac{R}{2T} (w^2 - x^2) - I_s y \quad (10)$$

Solving for y_{h_*} results in an explicit equation for this contour, corresponding to the water table head h_* (Figure 3) as a function of x :

$$\begin{aligned} y_{h_*}(x) &= \frac{R}{2TI_s} (w^2 - x^2) - \frac{h_*}{I_s} \\ &= a (w^2 - x^2) - \frac{h_*}{I_s}, \quad a = \frac{R}{2TI_s} \end{aligned} \quad (11)$$

For different values h_* , parabolic contours differ by distance from the upstream boundary ($y = 0$). Note that the coefficient a in the quadratic term of Equation 10 controls the contour curvature. Therefore, it is the critical term, relating groundwater recharge rate to the curvature of water table contours. The adjacent water table contours are identical in shape defined by Equation 11 and obtained by translation along the y -axis at distances $y > 0.5 w$.

Alternatively, distance D between the tip of parabola $y_{h_*}(0)$ and "base" of the parabola between streams $y_{h_*}(\pm w)$ or area under parabola A can be used to derive a :

$$D = y_{h_*}(0) - y_{h_*}(\pm w) = aw^2, \quad A = 4aw^3/3 \quad (12)$$

where any of two signs can be used.

Recharge Rate Evaluation from Contour Parameters

Recharge rate can be found using simple numerical or analytical procedures. In both cases, similar water table contours (roughly parabolic in shape) should be visually identified at some distance away from the upstream boundary and digitized.

In the numerical approach, parameter a is found by matching points along an entire digitized contour between streams (like in

Figure 1) to a parabola in Equation 11, resulting in recharge rate R :

$$R = 2a \cdot T \cdot I_s \quad (13)$$

In the analytical approach, parameter a can be found by two different ways. One is based on visual identification of parameter D and another is based on GIS-based evaluation of the area A between the contour and base (Figure 3).

In the first case (Analytical Approach A), values of parameters D and w yield parameter $a = D/w^2$ according to Equation 12. Substitution into Equation 13 results in explicit calculation of recharge rate:

$$R = \frac{2T \cdot I_s \cdot D}{w^2} \quad (14)$$

In the second case (Analytical Approach B), area A between the map contour and the base yields parameter $a = 3A/4w^2$ by Equation 12:

$$R = \frac{3}{2} \frac{A \cdot T \cdot I_s}{w^2} \quad (15)$$

Note that for the numerical approach, orientation of parabola axis may be non-collinear with x -axis due to deviations of local hydrogeological conditions from the model. For the first analytical approach, measurement of D at the exact midpoint between the streams may not capture the maximum curvature of the contour; for the second one, area-based approach, contour shapes may differ from parabola. The uncertainty of the recharge estimates will be discussed below based on comparisons between results from numerical and analytical approaches. Practical recommendations for calculating a and R using GIS are given and potential biases of the different approaches are discussed in more detail in Appendices B, C, and D.

Applications

Study Area

We calculated groundwater recharge rates in three regions in Nebraska, referred to as “Northern,” “Southern,” and “Eastern” regions (Figures 1 and 4). The regions are in locations where the aquifer is unconfined and two perennial streams are roughly parallel, approximating the assumptions used in deriving Equation 13. The Northern region encompasses roughly 3300 km² of the Loup River basin in the central Sand Hills. The Southern Region has an area of 2200 km² and lies in the Republican River basin, while the Eastern region encompasses 1500 km² in the Loup River basin. Average annual precipitation from 1981 to 2010 was 549, 540, and 684 mm year⁻¹ for the Northern, Southern, and Eastern regions, respectively (PRISM 2015). The surficial geology of the Nebraska Sand Hills extends slightly into the upstream portions of the Southern and Eastern regions and then transitions to loess in the downstream portions. All three regions overlie the High Plains aquifer.

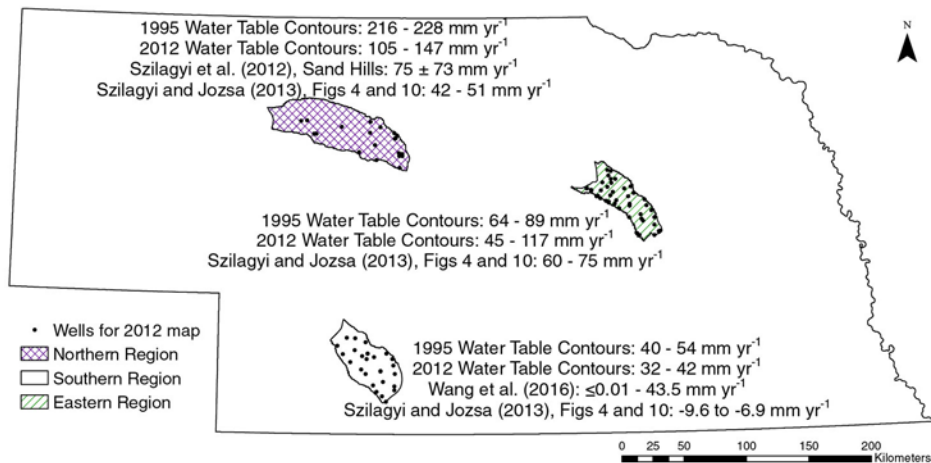


Figure 4. Water table contours used to estimate recharge in the Northern, Southern, and Eastern regions of Nebraska. Contours on the 1995 and 2012 maps are shown at 100 ft. (30.5 m) and 75 ft. (22.9 m) intervals, respectively. An example contour and curve fit from the Northern Region are also shown (note that axes showing curve fit are aligned with latitude and longitude, but rotated 90°; units are km). Multiple contours were analyzed and the mean recharge values are reported in Table 1 for each region and water table contour map.

Two previously published water table elevation maps were utilized. The first map used groundwater level data from spring of 1995. Manual interpolation techniques were applied mostly to 7.5 min maps, with hand-drawn contours in the vicinity of streams (Flowerday et al. 1998; Summerside et al. 2001). The second map interpolated groundwater levels mostly from spring seasons of 2009 to 2012 (6 out of the 91 measurements in our study regions were made during 2001 to 2008; A. Young, personal communication, 2018) using natural neighbor interpolation in ArcGIS software; minor corrections were made when groundwater elevation was greater than ground stream elevation etc. (A. Young, personal communication, 2017).

These two maps, referred to as 1995 and 2012 maps, respectively, were reasonably similar for the three regions analyzed in this paper (i.e., contours were oriented in a consistent direction, indicating a recharge area). Exact dates are not available for all groundwater level measurements, but the measurements were made in spring to allow groundwater levels to recover from seasonal pumping (e.g., in areas irrigated with groundwater) (Flowerday et al. 1998; Summerside et al. 2001). For instance, 99% of the measurements for the 2012 map occurred in the months of March or April. For all regions, accumulated precipitation over the 5 years prior to mapping (e.g., period of April 1, 2007 to April 1, 2012) was within 10% of long-term normal accumulation, with the exception of the Southern Region in 2012, which was 20% higher than long-term normal accumulation (climod.unl.edu, Northeast Regional Climate Center, supported by High Plains Regional Climate Center; accessed April 4, 2018). Differences between the two maps offered an opportunity to assess sensitivity of the proposed method to temporal changes in water table elevations, interpolation techniques, and different spatial density of groundwater levels used.

Data Analysis and Results

For each region, quadratic equations were fit to several water table contours (Figure 4) to find the coefficient a used in Equation 13 (numerical approach, Table 1). We also measured the dimensions of w and D (Equation 14; Analytical Approach A) and calculated area between each map contour and its base line (Equation 15; Analytical Approach B) to calculate a . Stream gradient I_s was determined from

Table 1. Recharge and Quadratic Coefficients from Numerical and Analytical (Analyt.) Approaches

Region	Date	Numerical ¹	Analyt. A ²	Analyt. B ³	Numerical	Analyt. A	Analyt. B
		R	R	R	<i>a</i>	<i>a</i>	<i>a</i>
		(mm year ⁻¹)			(km ⁻¹)		
Northern	1995	218	216	228	0.0467	0.0462	0.0488
Northern	2012	147	117	105	0.0325	0.0260	0.0233
Southern	1995	54	40	40	0.0323	0.0243	0.0241
Southern	2012	42	37	32	0.0276	0.0244	0.0214
Eastern	1995	89	64	72	0.0713	0.0510	0.0578
Eastern	2012	117	47	45	0.0910	0.0368	0.0349

1. Calculated using Equation 13.
2. Calculated using Equation 14.
3. Calculated using Equation 15.

a land surface digital elevation model (USGS 2017). Transmissivity T was based on existing saturated thickness (McGuire et al. 2012) and aquifer hydraulic conductivity data sets after Houston et al. (2013). Details of I_s and T calculations and values for each map region are included in Appendix E.

For the numerical approach, extracted points of groundwater elevation contours were plotted and a quadratic equation was fit to the data (Figure 4). On average, the 1995 contours for the three regions had slightly higher R^2 (0.89), compared to 0.86 for the 2012 contours. For Analytical Approach A, the distance $2w$ was measured between the water table contour—stream intersections for each contour. Then, starting at the midpoint between the two streams (i.e., distance w from the streams, Figures 2 and 3) the perpendicular distance between the “ $2w$ ” base line and the water table contour was measured. The values for w and D ranged from 8 to 18 km and 0.1 to 18 km, respectively. For Analytical Approach B, the area between the base line and the contour was calculated in ArcGIS[®], and values for A ranged from 0.7 to 454 km².

Recharge for the three regions and two maps was 95 mm year⁻¹, on average (based on both 1995 and 2012 maps, and both numerical and analytical approaches, $n=18$, Table 1). The Southern Region had the lowest recharge, on average (41 mm year⁻¹, $n=6$, Figure 5), which is consistent with lower long-term annual precipitation relative to the Northern and Eastern regions. The highest mean recharge

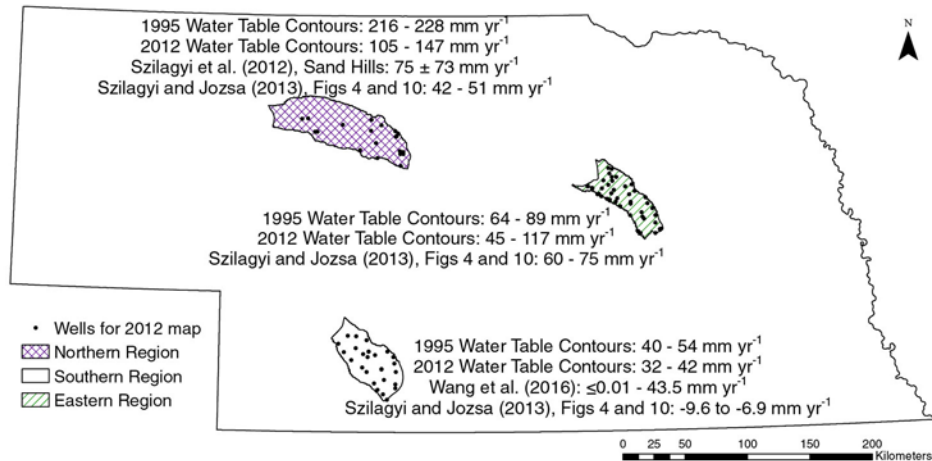


Figure 5. Comparison of mean recharge rates from water Table (WT) contours with previously published estimates. Note that values for Szilagyi et al. (2012) were for the entire Nebraska Sand Hills region, while values for Szilagyi and Jozsa (2013) were calculated from GIS raster files for their Figures 4 and 10. Locations where groundwater elevation was measured in each region (predominantly during years 2009 to 2012, for the 2012 water table map) are also shown.

was observed in the Northern Region (172 mm year⁻¹), consistent with very low surface water runoff in the Nebraska Sand Hills compared to the Eastern and Southern Regions (mostly dissected loess plains).

Online supporting information contains all w , D , A , and a values from analytical approaches and a and R^2 values from the numerical approach (Table S1, Supporting Information). Coefficients of variation for a in each region ranged from 23 to 73%, with an average of 42%. This variability highlights the benefit of estimating recharge based on several contours within a region, when possible. Supporting information (Figure S1) also includes illustrations of the quadratic curves with highest and lowest R^2 for each region, along with line segments showing D and w for the respective contours.

Discussion

Comparison with Other Methods

We compared recharge estimates for the three regions in this study to previously published recharge estimates (Figure 5), primarily

Szilagyi and Jozsa (2013), Szilagyi et al. (2012), and Wang et al. (2016). The statewide (1 km resolution) recharge maps of Szilagyi and Jozsa (2013) are based on evapotranspiration (ET) estimates, derived from moderate resolution imaging spectroradiometer (MODIS) and precipitation (P) data, with corrections for runoff. Szilagyi and Jozsa (2013, their figure 4) show P-ET values, while their figure 10 shows best estimates of recharge across the state, with uncertainty estimated at 10 to 15% of precipitation for the area of interest. Taking 12.5% of long-term average precipitation in our study regions gives ± 69 , ± 68 , and ± 86 mm year⁻¹ for Northern, Southern, and Eastern regions, respectively.

Overall, groundwater recharge rate estimates from water table contours appear reasonable, but mostly tend toward the upper limits of previous published estimates. Based on soil moisture measurements and inverse modeling, recharge estimates from Wang et al. (2016) were generally higher than from Szilagyi and Jozsa (2013). Similarly, groundwater recharge estimates from water table contours were generally high relative to mean values, but mostly within the range of values from Szilagyi and Jozsa (2013, their figures 4 and 10) for each respective region. Billesbach and Arkebauer (2012) approximated groundwater recharge of 115 ± 20 mm year⁻¹ at a research site roughly 10 km south of the Northern Region, and Wang et al. (2016) modeled 113 mm year⁻¹ at Arthur, NE (~60 km south), both similar to estimates from the 2012 water table contours (105 to 147 mm year⁻¹). For the Southern Region, Wang et al. (2016) found recharge rates of 43.5 mm year⁻¹ and < 0.01 mm year⁻¹ at the nearest Automated Weather Data Network Locations (McCook and Curtis, NE, respectively).

Comparison of Analytical and Numerical Approaches Applied to Two Different Water Table Maps

Despite the different potential biases for the three different approaches (Appendices C, D, and E), the coefficients of variation in R were mostly low. All regions had a coefficient of variation $\leq 17\%$, with the exception of the Eastern region (2012 map; 59%). The low variability in R between the different approaches suggests the methods used in this paper are robust, and uncertainty is on par with other recharge estimation methods.

Recharge estimates from the analytical approaches were lower than estimates from the numerical approach for all cases except the 1995 water table contours in the Northern Region. A key difference is that the numerical approach always integrates the maximum curvature of the water table contours (i.e., extreme values along the contour are accounted for as part of the least squares curve fitting), while Analytical Approach A (Equation 14) requires the variable D be measured at only one point. Due to irregularities along the water table contour, D may be underestimated in some cases (see Figure S1). Similarly, calculation of A for Analytical Approach B reflected contour irregularities that differed from the full parabolic shape predicted by the analytical model. For water table contours with significant irregularities, comparisons among numerical and analytical approaches are recommended to evaluate for potential biases or subjectivity of the method.

Of the three regions, the Northern Region has the lowest density of observation wells (**Figure 5**). For the 1995 water table contour map, only a handful of water table depths were measured in the Northern Region (the exact number was not published) and the hand-drawn water table contours (Summerside et al. 2001) follow intuitive, but possibly biased patterns in some areas. The difference in recharge estimates from the 1995 and 2012 water table maps suggests that even in areas where hydrogeology is sometimes viewed as relatively uniform (e.g., Nebraska Sand Hills), increased monitoring of groundwater elevations could be valuable.

Sources of Uncertainty to Consider in Future Studies

Appendices B through E include discussion of various sources of uncertainty related to the three different calculation approaches used in this study, and uncertainties in T and I_s . In addition, we note that this study was based on previously published groundwater elevation maps, which are the product of a long-term groundwater monitoring program that began in the 1950s (e.g., Reed 1956; Young et al. 2016). Transmissivity was determined from Houston et al. (2013) which relied on geologic exploration (including the large and systematic Nebraska Conservation and Survey Division Test Hole drilling program initiated in the 1940s) and subsequent interpretations that have been successfully used in calibrated and published groundwater models (e.g., Bitner 2005; Cannia et al. 2006; Stanton et al. 2010;

Rossman 2015). Clearly, many potential study sites will not have similar density of observations or previous published studies with which to gauge uncertainties. However, the potential uncertainty of any single variable in Equations 13 to 15 will map linearly to uncertainty in recharge (on a percentage basis, e.g., 20% error in hydraulic conductivity used to calculate T would result in 20% error in R), with the exception of the w_2 term. Below we explore potential uncertainty in one such term, D , due to the timing of groundwater level observations in irrigated areas. Similar exercises should be conducted when considering how data limitations or biases may affect recharge estimates at future study sites.

Effect of Water Table Seasonality

Given that a steady-state model was developed and applied in this study, use of a water table contour map developed from annually average groundwater levels would be ideal. However, even in Nebraska where groundwater level data is relatively abundant, high density regional well networks with long-term and frequent (e.g., daily) records are generally not available. Thus, we used existing water table contour maps based on spring-time water level measurements. However, if needed, the estimates of the potential bias in recharge resulting from water table elevation seasonality on recharge estimates can be assessed with Equation 14. Figure 6 depicts a change in D between springtime (D_{spring}) and late summer or early fall (D_{fall}), when groundwater is withdrawn from the area between the two streams. Annually averaged water table contours would likely fall between these two extremes.

The key question is the error in R resulting from changes in D (i.e., ΔD , shown in Figure 6). Consider recharge rates R_{spring} and R_{fall} corresponding to D_{spring} and D_{fall} , respectively. Equation 14 indicates that the relative errors in parameters R and D are identical:

$$\frac{R_{\text{fall}} - R_{\text{spring}}}{R_{\text{fall}}} = \frac{D_{\text{fall}} - D_{\text{spring}}}{D_{\text{fall}}} \quad (19)$$

Therefore, for an area where irrigation pumping occurs in the summer $\Delta D/D_{\text{fall}} = 50\%$ (or ΔD of approximately 2 km in the Southern Region, for example) would induce an equivalent bias of 50% in

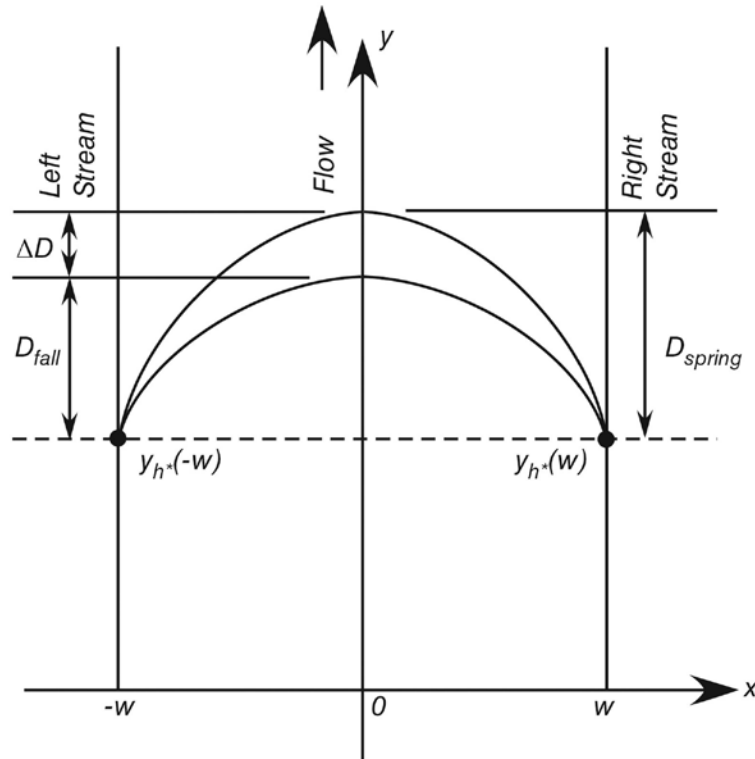


Figure 6. Example scenario where seasonal variation in groundwater levels could influence recharge estimates, using variable D from Equation 14 and Figure 3. Spring-time water table contours based on higher groundwater elevations, prior to aquifer drawdown from irrigation in the summer, may have greater length in the spring (D_{spring}) than groundwater elevations measured later in the year (D_{fall}).

calculated recharge rate. Assuming water levels are near steady state in the fall and in the spring, this crude estimate can assist in evaluating the sensitivity of recharge estimates to seasonality and can be used as a screening tool to determine applicability of the method in other study areas.

Conclusions

1. Water table patterns reflect the balance between recharge and discharge in areas with stream-aquifer interaction. In many cases, groundwater contours between streams display a parabolic convex shape over significant scales of space (e.g., 10 km and greater in this study) and time (e.g., months to years). The proposed

- approach to recharge estimation is based on a simple analytical model of groundwater flow between two parallel sloping stream segments (drainages). Assuming aquifer homogeneity, the model requires only three parameters, namely the aquifer transmissivity, the stream slopes, and the curvature or dimensions of water table contours between two streams.
2. Using GIS-based analysis, the method was applied for recharge estimation from two different water table maps for three regions in Nebraska. Application of three different approaches (one numerical and two analytical) gave consistent results, despite different potential sources of uncertainty or bias. Further, in spite of the simplicity of conceptual and mathematical models and some subjective elements in pattern recognition, calculated recharge rates were consistent with other studies, including those based on remote sensing estimates of evapotranspiration or inverse modeling based on field soil moisture time series.
 3. Considering its simplicity, this method may be a useful diagnostic tool for evaluation and clarification of regional water table maps by verifying consistency between transmissivity, sampling schedules, density of water table observations and, sometimes land surface DEM. This method can be applied to relatively small datasets and aid in prioritizing groundwater level monitoring programs. The simplicity of the model necessarily limits the hydrogeological settings where it may be applied. Our analyses produced reasonable recharge rates from real-world data from three regions in Nebraska, at least for the type of diagnostic applications described above.

Acknowledgments — This work was partially supported by the NSF (DGE-0903469) through funds awarded to V. Zlotnik through the IGERT program, USDA National Institute of Food and Agriculture (Hatch project NEB-21-177) to T. Gilmore, and the Daugherty Water for Food Global Institute at the University of Nebraska (student support to M. Johnson). We gratefully acknowledge A. Young and J. Szilagyi for groundwater elevation data for Nebraska and for GIS raster files used for figures 4 and 10) and J. Korus for discussion, all at SNR, UNL. Dr V.K. Boken, Department of Geography and Earth Science, University of Nebraska-Kearney contributed to the GIS pattern analysis at early stages of the work. Insightful comments by Dr Whittemore (KGS) and one anonymous reviewer contributed to the improved quality of the article.

Appendix A

Estimating the Correction $s(x, y)$

$$s(x, y) = -\frac{16Rw^2}{\pi^3 T} \sum_{n=0}^{\infty} \frac{(-1)^n \cos(\gamma_n x) e^{-\gamma_n y}}{(2n+1)^3}$$

$$\gamma_n = \frac{\pi(2n+1)}{2w} \quad (\text{A.1})$$

The locus of the largest absolute value of this function is at a point ($x = 0, y = 0$):

$$s(0, 0) = -\frac{16Rw^2}{\pi^3 T} \sum_{n=0}^{\infty} \frac{(-1)^n}{(2n+1)^3} \quad (\text{A.2})$$

Using Catalan's constant (Gradshteyn and Ryzhik 2000, Equation 6.234.3 and Equation 9.73),

$$G = \sum_{n=0}^{\infty} \frac{(-1)^n}{(2n+1)^3} \approx 0.915966 \quad (\text{A.3})$$

one obtains correction $s(x, y)$ along y -axis as follows:

$$\frac{s(0, y)}{s(0, 0)} = \frac{1}{G} \sum_{n=0}^{\infty} \frac{(-1)^n}{(2n+1)^3} e^{-\pi(2n+1)y/2w} \quad (\text{A.4})$$

For $y/2w > 0.25$, value of correction $s(x, y)$ is less than 1% of $s(0, 0)$ and can be neglected.

Appendix B

Calculating R Using Numerical Analyses and GIS

The algorithm requires finding a as follows:

1. Select an actual digital water table contour in ArcGIS.
2. Acquire coordinates (x,y) at contour points. We extracted coordinates at 10-m increments along the contour.
3. In Excel[®], fit $y = -ax^2 + bx + c$ to the contour points and find parameter a .
4. Using T and I_s found as described in Appendix E, and Equation 13 of the main text, calculate recharge rate for the selected contour.
5. Repeat the process for each contour, and calculate the mean R for the region.

Potential bias of the numerical approach may stem from the orientation of streams and/or groundwater flow patterns, which may not match expected coordinate systems (e.g., latitude and longitude). The water table contours in the three regions for this study were reasonably oriented to allow curve fitting (when longitude was plotted on the vertical axis, and latitude on the horizontal axis, to allow use of the standard trend line tool in Excel), but rotation of water table contours may be required in other studies. A potential advantage of the Numerical Approach is quantification of misfit between theoretical and actual contours (see R^2 values in Table S1 and Figure S1). Deviation from theoretical patterns could arise from violations of model assumptions (e.g., non-uniform recharge, perhaps from focused recharge through canals or dry channels, or other means).

Appendix C

Analytical Approach A to Determine R

1. For each water table contour, locate the two points of intersection with the stream.
2. Enclose the contour area by drawing a line segment (“base”) between the intersection points and calculating its length, $2w$.
3. Locate mid-point of the base.
4. Draw a normal from the mid-point of the base.
5. Calculate the intersection of the normal with the contour to determine the length D .
6. Use Equation 14 of the main text with T and I_s as described in Appendix E to calculate recharge rate for the selected contour.
7. Repeat the process for each contour and calculate the mean R for the region.

Potential bias from using analytical Approach A stems from bias in locating end points and measurement of width between streams because of (1) non-parallel streams, (2) equipotentials that deviate from predicted contour patterns, and (3) base lines that may not be normal to the streams. Additional uncertainty arises from visual identification of D , which may not intersect the contour at a representative distance from the base line. Of the three approaches, Analytical Approach A may be most sensitive to three-dimensional patterns of flow near streams, where water table contours may deviate from theoretical patterns. For Analytical Approach B and the Numerical Approach, these small deviations may be “averaged out” or have minimal effect on curve fitting and/or area calculations.

Appendix D

Analytical Approach B to Determine R

This approach includes the following steps:

1. Steps 1 to 2 from Analytical Approach A.
2. Calculate the areas enclosed by the base line and the contour in ArcGIS.
3. Use Equation 15 of the main text and T and I_s as described in Appendix E to calculate recharge rate for the selected contour.

Potential bias when using Analytical Approach B may result, as with Analytical Approach A, from uncertainty in the location of end points and measurement of width between streams.

Appendix E

Calculating IS and T and Associated Uncertainties

To define the three regions (Northern, Southern, Eastern), water table contours were clipped from the existing 1995 and 2012 water table maps in ArcGIS (Figure 4). Transmissivity (T) and stream slope (I_s) were then calculated for each region (Table E.1).

Stream gradient was calculated between upstream and downstream pairs of groundwater elevation contours (z_{up} and z_{down} , respectively) separated by distance between them d as follows

$$I_s = \frac{z_{up} - z_{down}}{d} \quad (\text{E.1})$$

where ground surface elevation, extracted from USGS (2017) at the intersection of a groundwater elevation contour and the stream (referred to here as “endpoints”). We note that the stream slope was estimated at larger length scale than a single meander and is likely greater than the actual slope of the streambed.

Transmissivity was estimated by multiplying spatially weighted average saturated hydraulic conductivity (K) and thickness (b):

$$T = K \cdot b \quad (\text{E.2})$$

Value b was area-weighted for each region:

$$b = \frac{\sum_{i=1}^n A_i \cdot b_i}{\sum_{i=1}^n A_i} \quad (\text{E.3})$$

where A_i is i -th area of the saturated thickness b_i , and n is the number of different areas in the region. Values for b_i and A_i were extracted from an existing polygon feature class (McGuire et al. 2012) with 30.5 m (100 ft) vertical resolution (for each thickness interval, b_i was taken as the mid-interval, e.g., for the 30.5 to 61 m thickness interval, $b_i = 45.8$ m). Spatially weighted average saturated thicknesses ranged from 220 m (standard deviation, $\sigma = 24$ m) in the Northern region, to 70 m ($\sigma = 34$) and 110 m ($\sigma = 43$ m) meters in the Southern and Eastern regions, respectively.

Spatially weighted average saturated hydraulic conductivity (K) values were based on existing hydraulic conductivity estimates from borehole data (Houston et al. 2013), which were interpolated using a spline with barriers (minimum curvature technique, Zoraster 2003). Values were extracted at 10-m intervals along each water table contour from interpolated K -surface, and the mean K value was calculated for each region.

Uncertainty in I_s and T from Spatial Variability was calculated for each region. The standard error (σ/\sqrt{n}) of I_s was calculated to evaluate uncertainty shown in Table E.1. Low variability in I_s suggests that the uniformity of slopes of the streams in each region was a reasonable approximation. For T , variability in K and b was propagated using the standard approach to uncertainty propagation (Taylor 1997). The uncertainty estimates are based strictly on variability in the various terms, and do not explicitly account for uncertainty in measurement techniques (e.g., possibly biased-high K if only production-well or irrigation-well geologic information is used) or the conceptual model assumptions used in deriving Equation 13 (i.e., “model error”).

Because saturated thickness b was spatially weighted (i.e., a weighted average) the weighted standard deviation was used, calculated as

$$\sigma_b = \sqrt{\frac{n'}{n' - 1} \cdot \frac{\sum_{i=1}^n A_i \cdot (b - b_i)^2}{\sum_{i=1}^n A_i}} \quad (\text{E.4})$$

where n' is the number of non-zero values of b_i (Heckert and Filliben 2003).

Table E.1. Transmissivity and Stream Slope for Each Region, with Uncertainties in Parentheses

<i>Region</i>	<i>Date</i>	T ($m^2 \text{ day}^{-1}$)	I_s ($\times 10^3$) ($m \text{ month}^{-1}$)
Northern	1995	2361 (186)	2.71 (0.17)
Northern	2012	2460 (217)	2.52 (0.23)
Southern	1995	824 (143)	2.77 (0.31)
Southern	2012	741 (203)	2.79 (0.42)
Eastern	1995	1050 (154)	1.63 (0.07)
Eastern	2012	1096 (160)	1.60 (0.09)

Authors' note — The authors have no conflicts of interest.

Supporting Information

Additional supporting information follows the **References**, including:

Table S1. Summary of Variables Calculated for the Numerical Approach and Analytical Approaches A and B, Including a , D , w . For the Numerical Approach, the R^2 value each curve fit is also shown.

Figure S1. Examples of quadratic curves fit to groundwater elevation contours. The best and worst curve fits are shown for each region.

References

- Anderson, M.P., and W.M. Woessner. 1992. *Applied Groundwater Modeling*, 381. San Diego, California: Academic Press, Inc.
- Bear, J. 1972 *Dynamics of Fluids in Porous Media*, 764. New York: American Elsevier New York.
- Billesbach, D.P., and T.J. Arkebauer. 2012. First long-term, direct measurements of evapotranspiration and surface water balance in the Nebraska Sand Hills. *Agricultural and Forest Meteorology* 156: 104–110. <https://doi.org/10.1016/j.agrformet.2012.01.001>
- Bitner, R.J. 2005. A groundwater model to determine the area within the Upper Big Blue Natural Resources District where groundwater pumping has the potential to increase flow from the Platte River to the underlying aquifer by at least 10 percent of the volume pumped over a 50 year period: Upper Big Blue Natural Resources District, p 24. <http://govdocs.nebraska.gov/epubs/N1500/B007-2005.pdf> (accessed April 9, 2018).
- Böhlke, J.K. 2002. Groundwater recharge and agricultural contamination. *Hydrogeology Journal* 10: 153–179. <https://doi.org/10.1007/s10040-001-0183-3>
- Bruggeman, G.A. 1999. In *Analytical Solutions of Hydrogeological Problems*, V. 46, Developments in Water Science, ed. G.A. Bruggeman. Amsterdam: Elsevier.
- Cannia, J.C., Woodward, D.W., and Cast, L.D. 2006. Cooperative Hydrology Study hydrostratigraphic units and aquifer characterization report: Cooperative Hydrology Study, p. 91. <https://digitalcommons.unl.edu/usgspubs/102/> (accessed April 9, 2018).
- Crosbie, R.S., P. Binning, and J.D. Kalma. 2005. A time series approach to inferring groundwater recharge using the water table fluctuation method. *Water Resources Research* 41, no. 1: W01008. <https://doi.org/10.1029/2004WR003077>

- Flowerday, C.A., R.D. Kuzelka, and D.P. Pederson. 1998. *The Groundwater Atlas of Nebraska*, 44. Lincoln, Nebraska: Conservation and Survey Division, Institute of Agriculture and Natural Resources, University of Nebraska Lincoln.
- Gradshteyn, I.S., and I.M. Ryzhik. 2000. *Table of Integrals, Series, and Products*, 6th ed., 1163. New York: Academic Press, Inc.
- Haitjema, H.M. 1995 *Analytic Element Modeling of Groundwater Flow*, 394. San Diego, CA: Academic Press, Inc.
- Haitjema, H. 2006. The role of hand calculations in ground water flow modeling. *Groundwater* 44, no. 6: 786–791. <https://doi.org/10.1111/j.1745-6584.2006.00189.x>
- Healy, R.W., and P.G. Cook. 2002. Using groundwater levels to estimate recharge. *Hydrogeology Journal* 10, no. 1: 91–109. <https://doi.org/10.1007/s10040-001-0178-0>
- Healy, R.W., and B.R. Scanlon. 2010. *Estimating Groundwater Recharge*, 245. Cambridge, UK: Cambridge University Press.
- Heckert, N. A. and Filliben, James J. (2003). NIST *Handbook 148: Dataplot Reference Manual, Volume 2: Let Subcommands and Library Functions*, National Institute of Standards and Technology Handbook Series, June 2003. <http://www.itl.nist.gov/div898/software/dataplot/document.htm> (accessed January 26, 2017)
- Hornero, J., M. Manzano, L. Ortega, and E. Custodio. 2016. Integrating soil water and tracer balances, numerical modelling and GIS tools to estimate regional groundwater recharge: Application to the Alcadozo aquifer system (SE Spain). *Science of the Total Environment* 568: 415–432. <https://doi.org/10.1016/j.scitotenv.2016.06.011>
- Houston, N.A., S.L. Gonzales-Bradford, A.T. Flynn, S.L. Qi, S.M. Peterson, J.S. Stanton, D.W. Ryter, T.L. Sohl, and G.B. Senay. 2013. Geodatabase compilation of hydrogeologic, remote sensing, and water-budget-component data for the High Plains aquifer. In *U.S. Geological Survey Data Series*, Vol. 777, 12. Reston, Virginia: U.S. Department of the Interior, U.S. Geological Survey.
- Huet, M., R. Chesnaux, M.-A. Boucher, and C. Poirier. 2016. Comparing various approaches for assessing groundwater recharge at a regional scale in the Canadian Shield. *Hydrological Sciences Journal* 61, no. 12: 2267–2283. <https://doi.org/10.1080/02626667.2015.1106544>
- Korus, J.T., L.M. Howard, A.R. Young, D.P. Divine, M.E. Burbach, J.M. Jess, and D.R. Hallum. 2013. *The Groundwater Atlas of Nebraska*, 3rd ed., Resource Atlas No. 4b/2013, 64. Lincoln, Nebraska: Conservation and Survey Division, School of Natural Resources, University of Nebraska-Lincoln.
- Lin, Y.-F., and M.P. Anderson. 2003. A digital procedure for ground water recharge and discharge pattern recognition and rate estimation. *Groundwater* 41, no. 3: 306–315. <https://doi.org/10.1111/j.1745-6584.2003.tb02599.x>
- Lin, Y.-F., J. Wang, and A.J. Valocchi. 2008. A new GIS approach for estimating shallow groundwater recharge and discharge. *Transactions in GIS* 12: 459–474. <https://doi.org/10.1111/j.1467-9671.2008.01113.x>
- McGuire, V.L., Lund, K.D., and Densmore, B.K. 2012. Saturated thickness and

- water in storage in the High Plains aquifer, 2009, and water-level changes and changes in water in storage in the High Plains aquifer, 1980 to 1995, 1995 to 2000, 2000 to 2005, and 2005 to 2009: U.S. Geological Survey Scientific Investigations Report 2012-5177, p. 28.
- Park, E. 2012. Delineation of recharge rate from a hybrid water table fluctuation method. *Water Resources Research* 48, no. 7: W07503. <https://doi.org/10.1029/2011WR011696>
- PRISM Climate Group 2015. *30-Year Normals (1981–2010)*. Oregon State University. <http://prism.oregonstate.edu> (accessed March 26, 2018).
- Reed 1956. Groundwater map of Nebraska showing relation of 1954 readings to median water level measurement. <http://snr.unl.edu/csd-esic/GWMapArchives/1954BW.jpg> (accessed April 4, 2018).
- Rossmann, N. R. 2015. Simulation of regional groundwater flow and the effects of future climate change on water resources in the Nebraska Sand Hills, *ETD Collection for University of Nebraska – Lincoln*. AAI3718064. <http://digitalcommons.unl.edu/dissertations/AAI3718064>
- Scanlon, B.R., R.W. Healy, and P.G. Cook. 2002. Choosing appropriate techniques for quantifying groundwater recharge. *Hydrogeology Journal* 10, no. 1: 18–39. <https://doi.org/10.1007/s10040-001-0176-2>
- Sophocleous, M. 1991. Combining the Soilwater balance and water-level fluctuation methods to estimate natural groundwater recharge - practical aspects. *Journal of Hydrology* 124, no. 3–4: 229–241. [https://doi.org/10.1016/0022-1694\(91\)90016-B](https://doi.org/10.1016/0022-1694(91)90016-B)
- Stanton, J.S., Peterson, S.M., Fienen, M.N. 2010. Simulation of groundwater flow and effects of groundwater irrigation on stream base flow in the Elkhorn and Loup River Basins, Nebraska, 1895-2055—Phase two: U.S. Geological Survey Scientific Investigations Report 2010–5149, p. 78.
- Stoertz, M.W., and K.R. Bradbury. 1989. Mapping recharge areas using a ground-water flow model—a case study. *Groundwater* 27: 220–228. <https://doi.org/10.1111/j.1745-6584.1989.tb00443.x>
- Su, N. 1994. A formula for computation of time-varying recharge of groundwater. *Journal of Hydrology* 160: 123–135.
- Summerside, S., M. Ponte, V.H. Dreeszen, S.L. Hartung, M.J. Khisty, and J. Szilagyi. 2001. *Update and Revision of Regional 1x2 Water-Table Configuration Maps for the State of Nebraska*, 9. Lincoln, Nebraska: Conservation and Survey Division – Institute of Agriculture and Natural Resources, University of Nebraska, Lincoln.
- Szilagyi, J., and J. Jozsa. 2013. MODIS-aided statewide net groundwater-recharge estimation in Nebraska. *Groundwater* 51, no. 5: 735–744. <https://doi.org/10.1111/j.1745-6584.2012.01019.x>
- Szilagyi, J., V.A. Zlotnik, J.B. Gates, and J. Jozsa. 2012. Mapping mean annual groundwater recharge in the Nebraska Sand Hills, USA. *Hydrogeology Journal* 19, no. 8: 1503–1513. <https://doi.org/10.1007/s10040-011-0769-3>

- Taylor, J.R. 1997. *An Introduction to Error Analysis*, 2nd ed. Herndon, Virginia: University Science Books.
- U.S. Geological Survey. 2017. 30-Meter digital elevation model, ArcGrid. <https://nationalmap.gov/3DEP/index.html>
- Vijay, R., N. Panchbhai, and A. Gupta. 2007. Spatio-temporal analysis of groundwater recharge and mound dynamics in an unconfined aquifer: A GIS-based approach. *Hydrological Processes* 21, no. 20: 2760–2764. <https://doi.org/10.1002/hyp.6487>
- Wang, T., T.E. Franz, W. Yue, J. Szilagyi, V.A. Zlotnik, J. You, X. Chen, M.D. Shulski, and A. Young. 2016. Feasibility analysis of using inverse modeling for estimating natural groundwater recharge from a large-scale soil moisture monitoring network. *Journal of Hydrology* 533: 250–265. <https://doi.org/10.1016/j.jhydrol.2015.12.019>
- Winter, T.O., J.W. Harvey, L.O. Franke, and W.M. Alley. 1998. *Groundwater and Surface Water, a Single Resource*. Denver, Colorado: U.S. Geological Survey Circular 1139.
- Wu, J., R. Zhang, and J. Yang. 1997. Estimating infiltration recharge using a response function model. *Journal of Hydrology* 198: 124–139.
- Young, A.R.; Burbach, M.E.; Howard, L.M.; Waszgis M.M.; Joeckel R.M.; Lackey, S.O. 2016. Nebraska Statewide Groundwater-Level Monitoring Report 2016. University of Nebraska–Lincoln, Conservation and Survey Division, Nebraska Water Survey Paper 84, p. 26.
- Zoraster, S. 2003. A surface modeling algorithm designed for speed and ease of use with all petroleum industry data. *Computers & Geosciences* 29, no. 9: 1175–1182. [https://doi.org/10.1016/S0098-3004\(03\)00139-0](https://doi.org/10.1016/S0098-3004(03)00139-0)

Table S1. Summary of Variables Calculated for the Numerical Approach and Analytical Approaches A and B, Including a , D , w . For the Numerical Approach, the R^2 value each curve fit is also shown.

Region	Date	Contour	Numerical	Numerical	Analyt. A	Analyt. A	Analyt. A	Analyt. B	Analyt. B
			a (km^{-1})	R^2 (-)	D (km)	w (km)	a (km^{-1})	A (km^2)	a (km^{-1})
Northern	1995	1*	0.0384	1.00	2.3	8.0	0.0350	25.0	0.0362
Northern	1995	2	0.0395	0.97	2.7	9.1	0.0322	35.2	0.0348
Northern	1995	3	0.0377	0.80	3.7	10.0	0.0364	62.1	0.0461
Northern	1995	4	0.0471	0.92	5.5	11.2	0.0442	90.8	0.0486
Northern	1995	5	0.0545	0.96	9.0	12.9	0.0539	150.9	0.0522
Northern	1995	6	0.0552	0.99	13.9	13.6	0.0754	183.7	0.0549
Northern	1995	7	0.0607	0.99	9.8	13.8	0.0515	215.7	0.0614
Northern	1995	8	0.0689	0.99	11.3	14.3	0.0550	271.8	0.0692
Northern	1995	9	0.0611	0.98	14.7	15.9	0.0583	319.4	0.0597
Northern	1995	10	0.0566	0.97	17.3	17.2	0.0586	381.7	0.0563
Northern	1995	11	0.0530	0.94	17.8	17.8	0.0564	408.2	0.0545
Northern	1995	12	0.0526	0.81	17.2	17.7	0.0548	447.5	0.0604
Northern	1995	13	0.0452	0.66	16.4	17.7	0.0520	453.7	0.0609
Northern	1995	14*	0.0369	0.63	13.7	16.8	0.0489	386.3	0.0615
Northern	1995	15	0.0442	0.94	13.5	17.5	0.0445	309.8	0.0437
Northern	1995	16	0.0387	0.87	10.4	16.5	0.0384	280.0	0.0470
Northern	1995	17	0.0310	0.82	8.3	16.8	0.0294	161.2	0.0257
Northern	1995	18	0.0344	0.89	6.3	14.9	0.0283	134.0	0.0304
Northern	1995	19	0.0316	0.91	5.0	14.2	0.0250	92.4	0.0243
Northern	2012	1	0.0765	0.92	3.0	9.5	0.0325	37.0	0.0319
Northern	2012	2	0.0250	0.82	2.5	10.3	0.0235	40.8	0.0277
Northern	2012	3	0.0225	0.97	3.4	12.8	0.0205	58.3	0.0207
Northern	2012	4	0.0302	0.99	4.8	14.5	0.0228	87.6	0.0215
Northern	2012	5	0.0289	0.86	8.5	17.0	0.0293	164.7	0.0251
Northern	2012	6	0.0296	0.89	8.5	17.6	0.0274	163.0	0.0223
Northern	2012	7	0.0453	0.87	10.6	17.6	0.0340	207.1	0.0283
Northern	2012	8	0.0337	0.77	8.1	17.7	0.0259	118.6	0.0161
Northern	2012	9	0.0214	0.85	8.2	18.0	0.0252	142.8	0.0183
Northern	2012	10	0.0375	0.86	9.4	16.6	0.0342	206.4	0.0338
Northern	2012	11	0.0284	0.90	7.6	16.9	0.0265	148.2	0.0230
Northern	2012	12	0.0276	0.98	6.1	15.9	0.0243	125.0	0.0235
Northern	2012	13	0.0165	0.99	1.2	10.0	0.0116	14.3	0.0106
Southern	1995	1*	0.0401	1.00	1.9	9.9	0.0193	22.9	0.0178
Southern	1995	2	0.0341	0.99	3.0	10.7	0.0259	44.1	0.0269
Southern	1995	3	0.0292	0.92	4.5	12.7	0.0275	79.0	0.0286
Southern	1995	4	0.0165	0.91	3.2	13.8	0.0168	71.4	0.0202
Southern	1995	5	0.0101	0.95	2.3	15.0	0.0103	63.6	0.0141
Southern	1995	6	0.0221	0.97	4.0	15.6	0.0162	90.2	0.0178
Southern	1995	7	0.0407	0.99	5.9	15.3	0.0250	112.7	0.0235
Southern	1995	8	0.0264	0.99	5.1	16.0	0.0199	91.5	0.0166
Southern	1995	9	0.0454	0.92	10.0	16.7	0.0359	206.1	0.0333
Southern	1995	10	0.0515	0.90	10.5	16.1	0.0402	213.6	0.0380
Southern	1995	11	0.0388	0.99	8.5	16.9	0.0300	179.5	0.0281
Southern	2012	1	0.0003	1.00	0.1	12.5	0.0008	0.8	0.0003
Southern	2012	2	0.0395	0.63	6.5	13.2	0.0374	71.6	0.0235

Region	Date	Contour	Numerical	Numerical	Analyt. A	Analyt. A	Analyt. A	Analyt. B	Analyt. B
			a (km^{-1})	R^2 (-)	D (km)	w (km)	a (km^{-1})	A (km^2)	a (km^{-1})
Southern	2012	3	0.0125	0.77	2.6	15.0	0.0115	58.7	0.0131
Southern	2012	4*	0.0262	0.49	8.5	14.7	0.0396	105.0	0.0250
Southern	2012	5	0.0313	0.94	4.5	16.3	0.0168	107.3	0.0185
Southern	2012	6	0.0558	0.82	10.3	16.0	0.0401	260.6	0.0477
Eastern	1995	1	0.1036	0.75	13.1	13.8	0.0683	268.6	0.0759
Eastern	1995	2	0.0978	0.81	10.3	14.8	0.0472	233.7	0.0546
Eastern	1995	3	0.1005	0.82	11.2	12.5	0.0718	240.9	0.0929
Eastern	1995	4	0.0318	0.93	3.9	12.3	0.0254	83.8	0.0335
Eastern	1995	5	0.0445	0.98	3.2	11.3	0.0251	50.6	0.0262
Eastern	1995	6	0.0189	0.63	3.2	9.4	0.0357	54.7	0.0488
Eastern	1995	7	0.0472	0.64	7.2	11.7	0.0524	121.8	0.0573
Eastern	1995	8	0.1262	0.80	10.5	11.3	0.0824	139.4	0.0730
Eastern	2012	1	0.1308	0.83	9.6	13.9	0.0498	196.3	0.0552
Eastern	2012	2	0.1473	0.90	7.0	13.9	0.0359	152.3	0.0421
Eastern	2012	3*	0.0858	0.99	3.3	12.2	0.0218	66.7	0.0273
Eastern	2012	4	0.0613	0.93	1.8	10.4	0.0170	29.6	0.0197
Eastern	2012	5	0.0424	0.93	4.8	11.7	0.0355	63.8	0.0301
Eastern	2012	6*	0.0784	0.61	8.5	11.8	0.0607	76.6	0.0350

Figure S1. Examples of quadratic curves fit to groundwater elevation contours. The best and worst curve fits are shown for each region.

